Preliminary study on the attenuation characteristics of ground motion recorded during the 2019 Ridgecrest earthquakes

Hongjun Si[1]; Kazuki Koketsu[2]; Hiroe Miyake[3]

[1]Earthquake Research Institute, University of Tokyo, Tokyo, Japan

Abstract

Two major earthquakes, the M_w6.5 and the M_w7.0 Ridgecrest earthquakes occurred about 200 km north-northeast of Los Angeles, California, at 10:33:49 on 4 July and 20:19:53 on 5 July 2019 (PDT), respectively. In this study, we compare the attenuation characteristics of the strong ground motions of the two earthquakes with the existing GMPEs developed in Japan and the United States, and investigate the spatial distribution of the observed ground motions.As the preliminary results, we compared the PGAs and PGVs observed during the two Ridgecrest earthquakes and the GMPE by Si and Midorikawa (1999), and found that, (1) the observed PGAs for both M_w6.5 and the M_w7.0 earthquakes are generally consistent with the predictions; (2) For PGV, the observations are generally also consistent with the predictions, while at distances around 180-200 km, some of the PGVs observed in Los Angeles downtown area are relatively larger than the predictions by GMPE.

Data and Methodology

Data

The ground motion data used in this study are those compiled by CESMD. Among these data, the records observed at the stations installed in buildings were excluded. The closest distance from the seismic faultto an observation station is defined as the source distances. PGA and PGV are defined as the larger one among the PGAs and PGVs of the two horizontal components. M_w estimated by GCMT are used in the analysis. PGV are defined as the larger one among the PGAs and PGVs of the two horizontal components. M_w estimated by GCMT are used in the analysis.

Method

The GMPE used in the analysis is that proposed by Si and Midorikawa (1999, 2000, refer to as SM99 model hereafter) which were developed based on the database derived in Japan, including earthquakes with a range of moment magnitudes covered from 5.8 to 8.3. In their models, PGA is defined on free surface and PGV is defined on bedrock with a shear wave velocity of about 600 m/s. The earthquakes are classified into three types, that is, crustal, inter-plate and intra-plate earthquakes. SM99 models are shown in following Eqs.

$$\log PGA = 0.50\,M_w + 0.0043D + d - \log(X + 0.0055 \cdot 10^{0.5\,M_w}) - 0.003\,X + 0.61$$

$$\log PGV = 0.58\,M_w + 0.0038D + d - \log(X + 0.0028 \cdot 10^{0.5\,M_w}) - 0.002\,X - 1.29$$

where X, M_w show fault distance, and moment magnitude, respectively. D is focal depth, represented by the depth of the center of a fault plane. d shows the coefficient for earthquake types: 0.0 for crustal, -0.02 and 0.12 for inter- and intra-plate events, respectively. Si et al. (2010) have compared SM99 with strong motion data recorded during the 1994 Northridge, and found that they are generally consistent, as shown in Figure 1.

In this study, we check if the strong motion data in the 2019 Ridgecrest earthquake sequences consistent with SM99. Then we calculated the residuals between SM99 and the observations to check its spatial distribution.

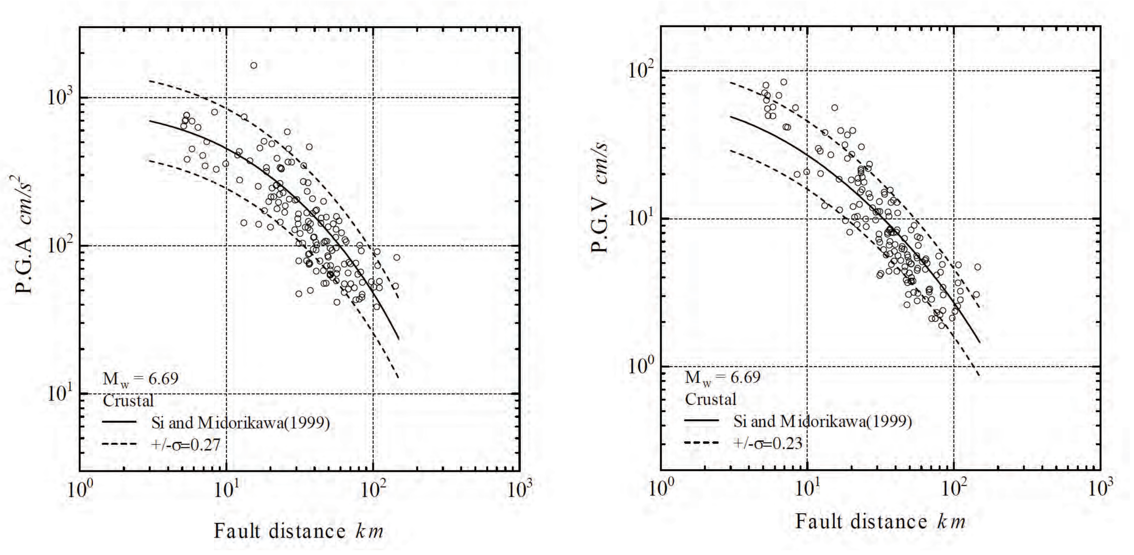

Figure 1. Attenuation characteristics of peak values for the 1994 Northridge earthquake and the prediction by reference model proposed by Si and Midorikawa (1999) (Left: PGA, right: PGV, after Si et al., 2010)

Results (1/2)

Results for the M6.4 earthquake

Figure 2 shows the comparison between the observed PGA and PGV and the predictions by SM99. In the calculation of SM99, we used the a M_w of 6.5 based on the result by GCMT. For PGV, since no sufficient data of Vs30 for the obersion stations, the predictions are plotted for Vs30=200 m/s and 600 m/s, respectively. The results show that, for PGA, the observations are generally consistent with the predictions. For PGV, it can be confirmed that the observations show the same attenuation tendency with SM99. Figure 3 shows the spatial distribution of residual between observation over SM99. For PGV, preduction is for soil with Vs30=300 m/s. The results show that the ground motion recorded at the observation stations in Los Angeles area tends to be larger than the predictions by SM99.

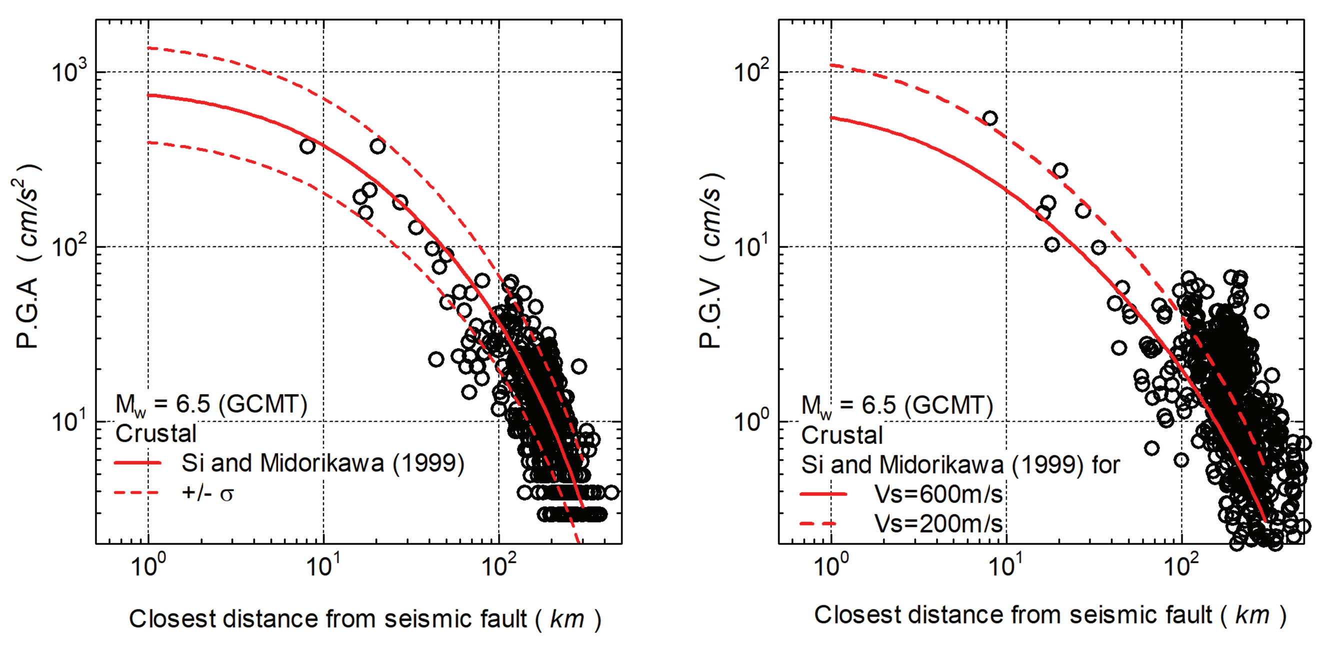

Figure 2. Comparison between the observed PGA and PGV and the predictions by SM99 for the M6.4 earthquake.

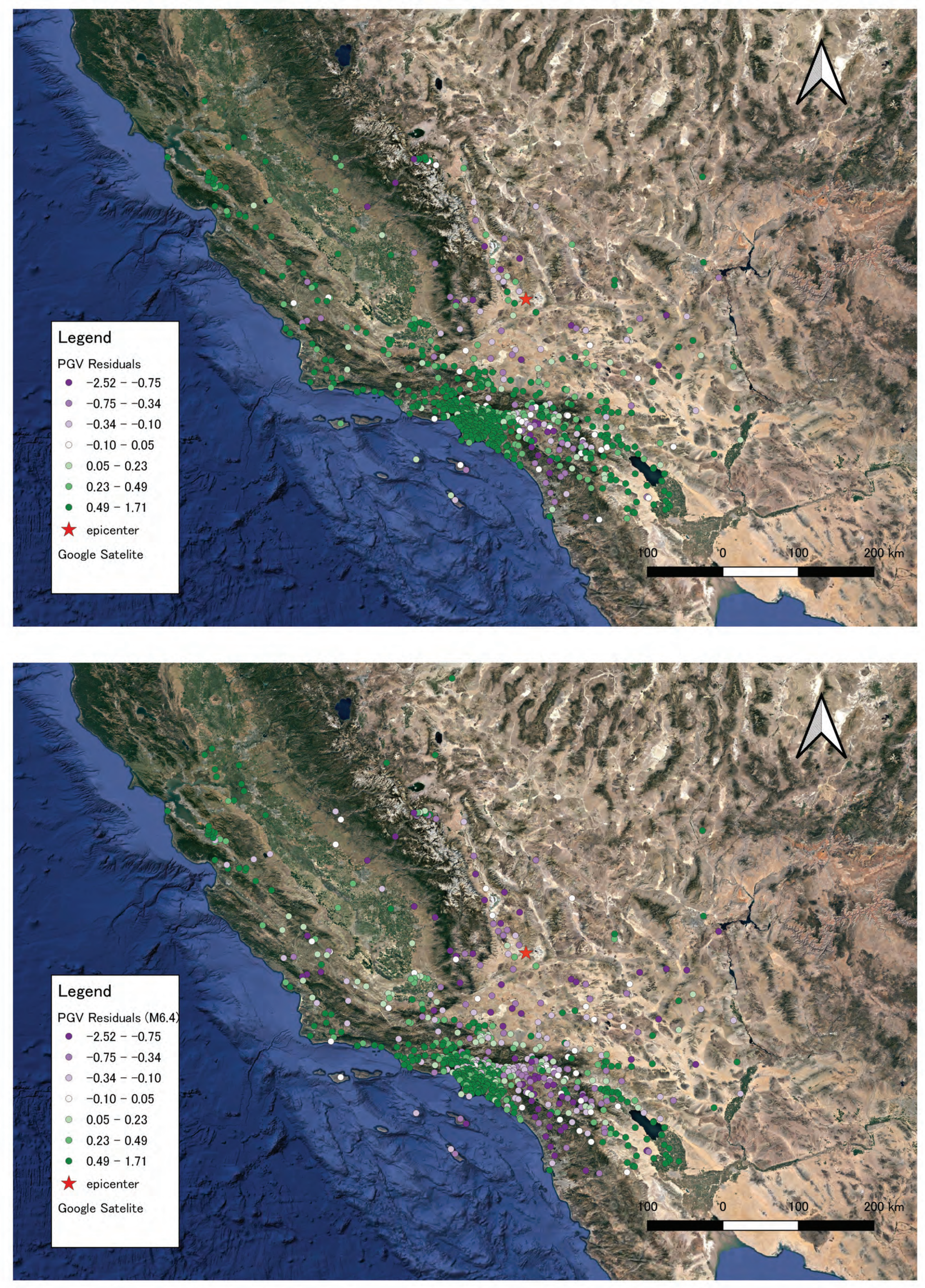

Figure 3. Spatial distribution of residuals between the observed PGAs (upper), PGVs (lower) and the predictions by SM99 for the M6.4 earthquake.

Results (2/2)

Results for the M7.1 earthquake

Figure 4 shows the comparison between the observed PGA and PGV and the predictions by SM99. In the calculation of SM99, we used the a M_w of 7.0 based on the result by GCMT. For PGV, since no sufficient data of Vs30 for the obersion stations, the predictions are plotted for Vs30=200 m/s and 600 m/s, respectively. The results show that, for PGA, the observations are generally consistent with the predictions. For PGV, it can be confirmed that the observations show the same attenuation tendency with SM99. Figure 5 show the spatial distribution of residual between observation over SM99. For PGV, preduction is for soil with Vs30=300 m/s for Vs30=300 m/s. Also, the results show that the ground motion recorded at the observation stations in Los Angeles area tends to be larger than the predictions by SM99.

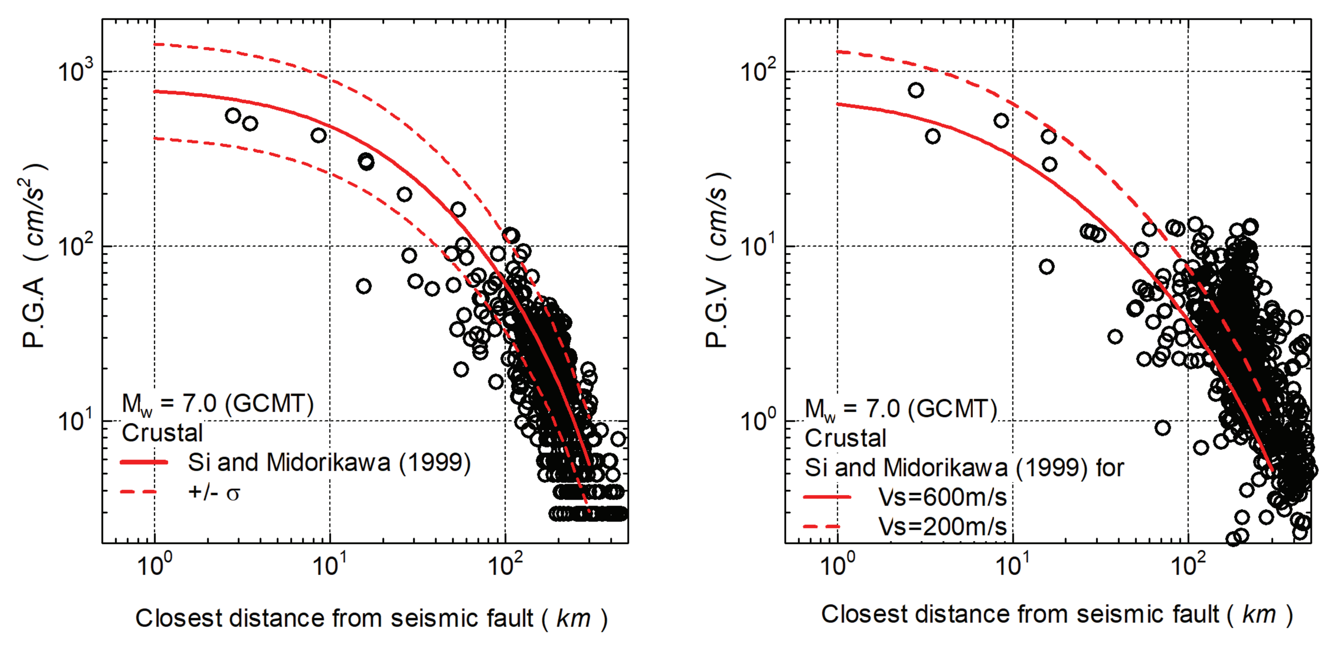

Figure 4. Comparison between the observed PGA and PGV and the predictions by SM99 for the M7.1 earthquake.

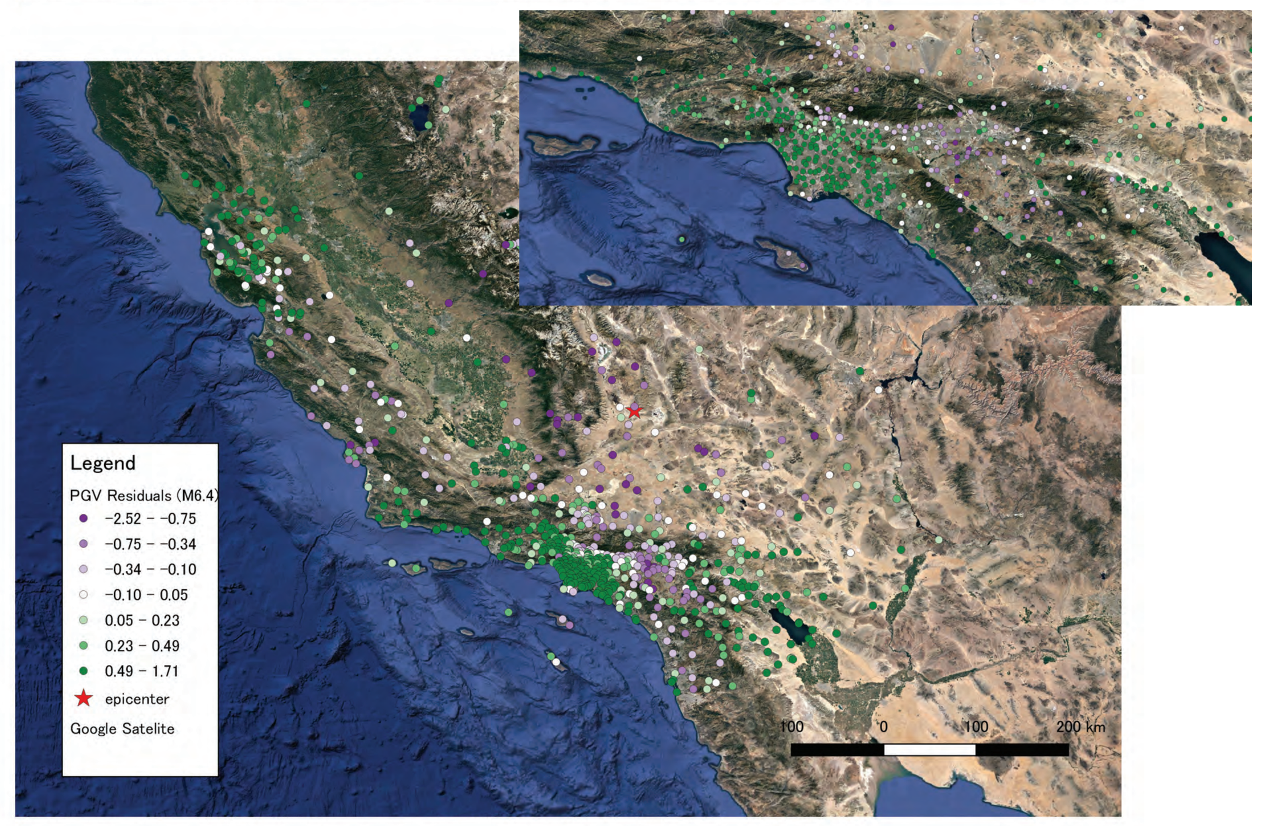

Figure 5. Spatial distribution of residuals between the observed PGAs (upper), PGVs (lower) and the predictions by SM99 for the M7.1 earthquake.

References

(1) Si, H., & Midorikawa, S. (1999). New attenuation relationship for peak ground acceleration and velocity considering e ects of fault type and site condition. Journal of Structural and Construction Engineering AIJ, 523, 63–70. (in Japanese with English Caption and Abstract). (2) Si, H., Tsutsumi, H., & Midorikawa, S. (2010). Evaluation of hanging wall e ects on ground motion attenuation relationship correcting the site e ects. In Proceedings of the 9thNCEE/10CCEE. Paper No.467. (3) The Center for Engineering Strong Motion Data (CESMD): https://strongmotioncenter.org/.

Acknowledgments

The authors thank the Center for Engineering Strong Motion Data (CESMD) provides the strong motion data. QGIS and data of Google Satellite are used to plot maps.